Diradicals Photogeneration from Chloroaryl-Substituted Carboxylic Acids

Lorenzo Di Terlizzi,[a] Stefano Protti,[a] Davide Ravelli,[a] and Maurizio Fagnoni*[a]

Abstract: With the aim of generating new, thermally inaccessible diradicals, potentially able to induce a double-strand DNA cleavage, the photochemistry of a set of chloroaryl-substituted carboxylic acids in polar media was investigated. The photoheterolytic cleavage of the Ar–Cl bond occurred in each case to form the corresponding triplet phenyl cations. Under basic conditions, the photorelease of the chloride anion was accompanied by an intramolecular electron-transfer from the carboxylate group to the aromatic radical cationic site to give a diradical species. This latter intermediate could then undergo CO_2 loss in a structure-dependent fashion, according to the stability of the resulting diradical, or abstract a hydrogen atom from the medium. In aqueous environment at physiological pH (pH = 7.3), both a phenyl cation and a diradical chemistry was observed. The mechanistic scenario and the role of the various intermediates (aryl cations and diradicals) involved in the process was supported by computational analysis.

Introduction

Diradicals are key intermediates in synthesis[1,2] and medicinal chemistry, being often implicated in the mechanism of action of several antitumorals.[3] However, the generation of species featuring the concomitant presence of two unpaired electrons is not always a straightforward process.[1] Such intermediates can be obtained either thermally or photochemically, but the latter approach, as largely documented,[4] is more versatile and found widespread use in photoeliminations (e.g. photoextrusions or the formation of o-benzynes) and in Norrish type I/II reactions.[4,5] As mentioned, diradicals may have a role even in biology.[3] A prototypical case is that of p-benzynes (σ,σ-diradicals) generated from antitumor antibiotics, such as enediyne-based Dynemicin A,[3b] able to abstract hydrogen atoms from DNA, thus leading to double-strand DNA cleavage.[3c,6] Neocarzinostatin, another enediyne antibiotic, first binds to DNA and then, after a nucleophilic attack by the thiol group of glutathione, rearranges to form an enyne-[3]-cumulene prone to give an aggressive 1,5-didehydro indene diradical through the so called Myers-Saito cycloaromatization.[2a,7] In some instances, the latter process was found to occur also under photochemical conditions.[4] The success of this approach for DNA cleavage relies on the formation of highly aggressive species eager to take hydrogen atoms. One interesting option in this field is the use of anticancer prodrugs that photorelease aggressive species at will upon light exposure.
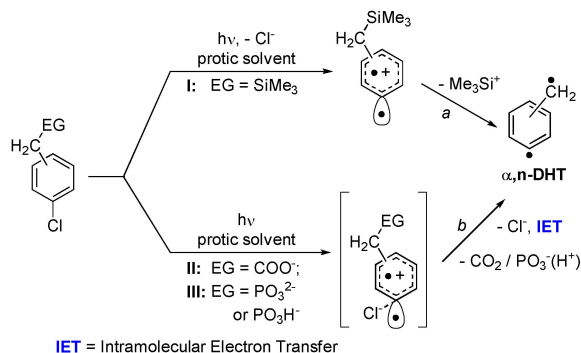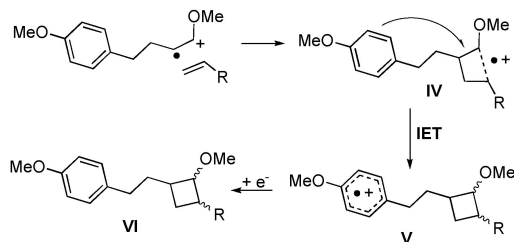
Accordingly, the design of routes enabling the photogeneration of (new) diradicals, alternative to thermal pathways, is highly desirable. A good starting point is the thermal Myers-Saito reaction used to generate α,3-didehydrotoluenes (α,3-DHTs, heterosymmetric σ,π-diradicals) from polyunsaturated species.[2a] In fact, our group found that the very same intermediates can be formed, even in aqueous phosphate buffer solution (PBS, pH = 7.3), by a one-photon double-elimination reaction starting from an aromatic derivative. Notably, this approach could be extended to the photogeneration of all α,n-DHT (n = 2–4) isomers (Scheme 1a).[8,9] This process is based on the photoheterolytic elimination (via a C(sp²)-X bond cleavage) of a nucleofugal group (usually, the chloride anion) from the aromatic ring followed by the detachment of a stable electrofugal group (EG, such as the trimethylsilyl cation,[8a–c] carbon dioxide[8d] or a metaphosphate anion[9]) from the benzylic position of the resulting phenyl cation. Intriguingly, a different reaction course has been identified, depending on the actual electrofugal group. The loss of the Me_3Si^+ moiety occurs spontaneously, thanks to the peculiar stabilization of the positive charge offered by the silicon atom (Scheme 1a, path a).[8a–c,10] An initial intramolecular electron transfer (IET) process occurring at the triplet phenyl cation stage operates, however, in the formation of α,n-DHTs when a negatively charged electrofugal group is involved (–COO^- or –PO_3^{2-}/–PO_3H^-, Scheme 1a, path b).

However, α,n-DHTs cannot be considered aggressive diradicals, since the unpaired electron at the benzylic site is stabilized by resonance and this site is thought to be inefficient in the abstraction of a hydrogen atom from the medium, accordingly. Moreover, we found that changing the methylene group with a heteroatom failed to induce the generation of the corresponding (hetero)diradical.[11]
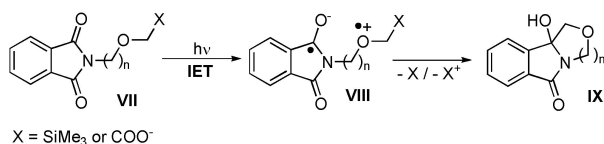
[a] L. Di Terlizzi, Prof. S. Protti, Prof. D. Ravelli, Prof. M. Fagnoni
     PhotoGreen Lab
     Department of Chemistry
     V. Le Taramelli 10, 27100 Pavia (Italy)
     E-mail: fagnoni@unipv.it

Chemistry–A European Journal

Research Article
doi.org/10.1002/chem.202200313

Chemistry Europe
European Chemical
Societies Publishing

Scheme 1. Literature precedents relevant to the present investigation.

We, reasoned that an IET could be the key to devise new, interesting diradical intermediates, endowed with a tunable character in terms of stabilization/reactivity. As a matter of fact, electron transfer reactions are quite common in biological systems.[12] In some cases, the intramolecular version of this phenomenon is invoked to explain the outcome of a given photochemical reaction, either in synthetic endeavors or in the biological environment,[13] and may take place even at long-range distance.[14] The success of some photochemical reactions is based on IET, where an easily oxidizable (or reducible) moiety is purposely tethered to the reacting system to donate (accept) an electron to (from) a radical cationic (anionic) site in a remote part of the molecule, thus allowing the formation of the desired product. This moiety is sometimes called redox-tag,[15] as in the case of the $MeOC_6H_4$ group in the photochemically generated intermediate **IV**: it initially underwent an IET to afford **V** and then was restored, allowing the formation of compound **VI** (Scheme 1b). A radical ions couple may be alternatively formed upon (photoinduced) IET. An exemplary case is that of substituted phthalimides **VII** (Scheme 1c), wherein an IET leads to the formation of two radical ion centers (see **VIII**). Thus, the radical cation site triggers a desilylation (or decarboxylation), allowing the thus formed radical-radical ion couple to undergo cyclization to finally release tricyclic compound **IX**.[16]

As for the above, we envisaged that a thermal IET process on a photogenerated intermediate may induce the generation of a new class of (potentially aggressive) diradicals. The designed models (chloroaromatics **X**, Scheme 2) feature the presence of a carboxylate moiety in the double role of electron donor and electrofugal group, and can benefit ofits good oxidizability, biological compatibility and simplicity of installation in the desired substrate. A purposely designed X–Y spacer then separates the COOH moiety from the aromatic ring. If a triplet phenyl cation (see intermediate **XI**) is formed upon photolysis of **X**, the occurrence of an IET would give **XII**, an aggressive diradical able to abstract two hydrogen atoms from the medium to give **XIII** via the formation of strong bonds (Ar–H and COO–H). Alternatively, carbon dioxide loss from **XII** to form diradicals **XIV** is another interesting issue, since it could open the route to an unexplored class of diradicals, which reactivity is virtually unknown and worth to be investigated.

Results

Experimental data

To test our idea, we investigated the photochemistry of compounds **1a**–**e** (Figure 1). Carboxylic acids **1a** and **1e** were commercially available, whereas compounds **1b**–**d** were readily
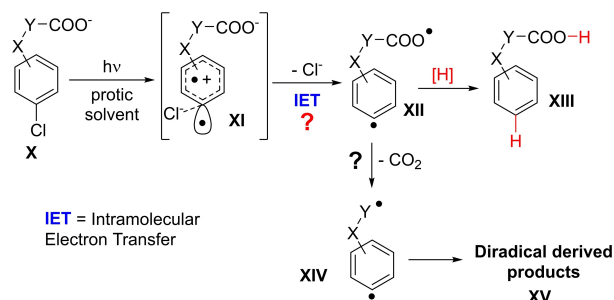
Scheme 2. Proposed approach for the formation of diradicals based on Intramolecular Electron Transfer (IET).

1a

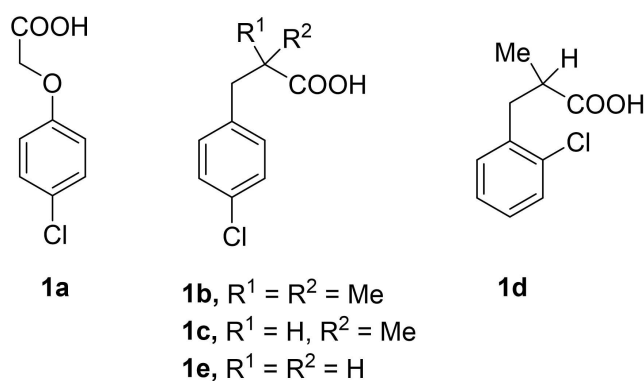**1b**, R^1 = R^2 = Me
1c, R^1 = H, R^2 = Me
1e, R^1 = R^2 = H

1d

Figure 1. Structures of compounds **1a–e**.

Chemistry–A European Journal

Research Article
doi.org/10.1002/chem.202200313

Chemistry Europe
European Chemical
Societies Publishing

synthesized by following known procedures (see Experimental section and Supporting Information for further details).

The fluorescence quantum yields for aryl propionic acids **1b–e** are very low ($\Phi_F < 0.01$), both in the protonated and in the deprotonated form (**1′b–e**). Slightly higher values have been determined for 4-chlorophenoxyacetic acid **1a** and its carboxylate anion **1′a** ($\Phi_F = 0.021$ and 0.019, respectively).

The photochemical reactions were carried out by direct irradiation (centered at 254 nm, coming from low pressure Hg vapor lamps) in different polar protic media, including neat *i*PrOH, MeOH and an aqueous phosphate buffer solution at physiological pH (7.3) to facilitate the photoheterolytic cleavage of the Ar–Cl bond. 4-Chlorophenoxyacetic acid **1a** was first tested for different reasons. First, the anisole-like structure of this compound assures an easy photogeneration of the corresponding triplet phenyl cation.[17] Second, this is a good candidate to investigate the proposed IET process occurring in zwitterion **XI**, since the resulting diradical **XII** should be quite prone to lose carbon dioxide due to the stability of the corresponding diradical **XIV**. In fact, the phenoxymethyl radical has been already described in the *O*-neophyl rearrangement of 1,1-diarylalkoxy radicals[18] and directly detected by laser flash photolysis of anisole in solution.[19] Moreover, the photosensitized decarboxylation of acids of general formula ArXCH$_2$COOH (X=O, S) has been previously documented.[20]

Thus, irradiation of **1a** in different polar media gave a varied products distribution (see Table 1), showing a markedly differ-

ent behavior when moving from the free acid (**1a**) to the corresponding carboxylate anion (**1′a**). The photoproducts formed by irradiation of **1a** may be classified in two main families, namely chlorine-free products (**2–4**) and carboxylate/chlorine-free derivatives (products **5–7**). A set of photochemical experiments were first carried out in alcoholic solvents under base-free conditions (0.01 M **1a**) upon a 60–120 min period. Thus, irradiation in neat *i*PrOH led to the exclusive formation of photodechlorinated phenoxyacetic acid **2** (Table 1, entry 1), even when using acetone-sensitized conditions (in this case the irradiation wavelength was centered at 310 nm by means of low pressure phosphor-coated Hg vapor lamps; entry 2).[17] In MeOH, the consumption of **1a** was almost quantitative (entry 3) and **2** was again the main photoproduct along with a small amount of 2-(4-methoxyphenoxy)acetic acid **3**. Similar results were obtained when carrying out the reaction by using 0.02 M **1a** (entry 4) or under sensitized conditions (entry 5). Adding one equivalent of base (Cs$_2$CO$_3$, 5×10^{-3} M) in the experiments in MeOH made the consumption faster ($\Phi_F = 0.18$) and drastically changed the products distribution. In fact, the irradiation of **1a** under such conditions gave only carboxylate/chlorine-free products, including phenoxyethanol **5** and 1,2-diphenoxyethane **6**, independently of the concentration used (entries 6 and 7).

On the route towards physiological conditions, we tested the photoreactivity of **1a** in phosphate buffered solution (PBS, pH = 7.3)/MeOH 1:1. The irradiation in this aqueous-alcoholic

Table 1. Photochemistry of 4-chlorophenoxyacetic acid **1a** in polar media.[a]

Entry	Conditions [Φ_{-1}][b]	Time [min]	1a Consumption [%]	Products, yield [%][c]
1	*i*PrOH (0.02)	120	85	**2**, 59
2	*i*PrOH[d]	120	40	**2**, 70
3	MeOH (0.07)	120	94	**2**, 62; **3**, 7
4	MeOH[e]	120	46	**2**, 20; **3**, 11
5	MeOH[d]	120	50	**2**, 28; **3**, 6
6	MeOH + Cs$_2$CO$_3$ (1 equiv.) (0.18)	60	100	**5**, 49; **6**, 7
7	MeOH[e] + Cs$_2$CO$_3$ (1 equiv.)	60	97	**5**, 54; **6**, 16
8	MeOH:PBS[f] 1:1	90	87	**2**, 5; **3**, 2; **4**, 5; **5**, 46; **6**, 1; **7**, 9
9	PBS[f] (0.07)	90	62	**2**, 10; **4**, 44; **6**, 5; **7**, 40
10	PBS[f] + Glucose (0.05 M)	120	96	**2**, 23; **4**, 23; **7**, 52; **6**, 2
11	PBS[d,f]	60	68	**2**, 25; **4**, 16; **7**, 28; **6**, 3
12	PBS[d,f,g]	60	88	**2**, 16; **4**, 11; **7**, 32; **8** + **9**, traces[h]
13	CD$_3$OD, + Cs$_2$CO$_3$ (1 equiv.)	120	100	**5-d$_3$**, 54; **6-d$_2$**, 12

[a] Irradiations were performed at 254 nm (8×15 W low pressure Hg vapor lamps) on a nitrogen-saturated 0.01 M solution of **1a** in the examined solvent. [b] Determined at λ=254 nm. [c] Yields based on consumed **1a**. [d] Irradiations performed at 310 nm (8×15 W phosphor coated Hg lamps) in the presence of acetone (20 %v/v). [e] 0.02 M **1a**. [f] Phosphate buffer solution (PBS) 0.05 M, pH=7.3. [g] Reaction carried out in the presence of *t*butyl acrylate (2 equiv.). [h] Compounds **8** and **9** detected by GC/MS analysis.

Chemistry–A European Journal

Research Article
doi.org/10.1002/chem.202200313

Chemistry Europe
European Chemical
Societies Publishing

solution gave a complex mixture, with an overall predominance of carboxylate/chlorine-free products, being **5** the compound formed with the highest yield (entry 8). Irradiation of **1a** in neat PBS gave roughly an equimolar amount of chlorine-free and carboxylate/chlorine-free derivatives (**4** and **7** as the major products, respectively, entry 9) that was slightly affected by the presence of 0.05 M glucose (entry 10).[9] Shifting the irradiation wavelength to 310 nm led to the same products (entry 11), while the addition of *t*butyl acrylate (2 equiv.) as radical trap led to the formation of adducts **8** and **9** in trace amounts, as detected by GC-MS analysis (entry 12). Finally, irradiation of **1a** in CD₃OD in the presence of 1 equiv. of Cs_2CO_3 caused the formation of phenoxyethanol containing three deuterium atoms (**5-d_3**) or led to dimer **6-d_2** (entry 13), as revealed by GC-MS analysis (see Scheme S6 in the Supporting Information for further details). The product distribution closely resembled that obtained in basic MeOH (entry 6).

Next, we shifted our attention to **1b** to evaluate the feasibility of the decarboxylation step at the phenyl cation level towards the formation of a tertiary radical (Table 2). Irradiation in neat MeOH did not afford any decarboxylated species, since only photodechlorinated 3-phenyl-2,2-dimethylpropionic acid **10** and 3-(4-methoxyphenyl)-2,2-dimethylpropionic acid **11** were formed. The consumption quantum yield ($\Phi_F = 0.02$) was quite low and unreacted **1b** (37%) has been detected after 2 h irradiation (entry 1). When switching to basic methanol, acid **10** remained the main product, but it was accompanied by carboxylate/chlorine-free derivatives, namely 3,3-dimethyl-4-phenylbutan-1-ol **13**, (2-methoxy-2-methylpropyl)benzene **14** and traces of (2,2,3,3-tetramethylbutane-1,4-diyl)dibenzene **15**, according to GC-MS analysis (entry 2). Buffered water improved the photoreactivity of **1b** ($\Phi_F = 0.12$) and dechlorinated **10** was by far the major product along with solvent-incorporating product 3-(4-hydroxyphenyl)-2,2-dimethylpropionic acid **12** (entry 3). Dimer **15** (formed in trace amounts) was the only carboxylate/chlorine-free derivative detected.

We then considered α-benzyl propionic acid isomers **1c** and **1d** (Table 3). As a matter of fact, irradiation of **1c** in methanol even in the presence of Cs_2CO_3 (1 equiv., 5×10^{-3} M) gave 3-phenyl-2-methylpropionic acid **16** as the sole product (entries 1, 2). Experiments in PBS were not performed with this substrate, due to solubility problems of **1c** in this medium. Photolysis of **1d** (5×10^{-3} M) in (basic) MeOH consistently led to **16** (entry 4), whereas in PBS (with the help of 5% MeCN for solubility reasons) the photodechlorinated acid was accompanied by a significant amount of 3-(2-hydroxyphenyl)-2-methylpropionic acid **17** (entry 5). However, no products deriving from a double chlorine/carbon dioxide elimination were formed.

The last carboxylic acid tested was 3-(4-chlorophenyl)propionic acid **1e** (Table 4). Experiments were again carried out in methanol, methanol with 1 equiv. of Cs_2CO_3 (5×10^{-3} M) and buffered water at physiological pH of 7.3 (PBS) with 5% MeCN. In all solvents tested, the major product was 3-phenylpropionic acid **18** along with the photosolvolysis products 3-(4-methoxyphenyl)propionic acid **19** and 3-(4-hydroxyphenyl)propionic acid **20**.
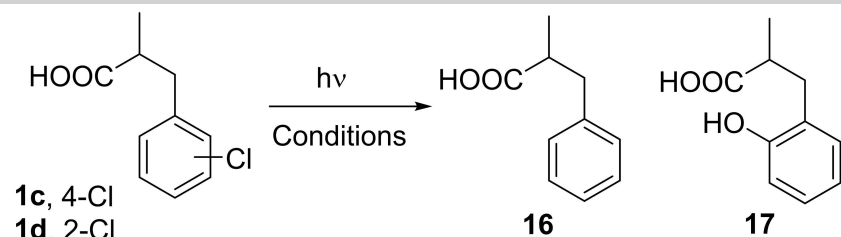
Computational data

To get additional insights into this multi-faceted photochemical reactivity, we complemented the experiments carried out on **1a–e** with a computational investigation on each of the relevant steps of the process. The aim was to showcase the validity of our initial hypothesis about the key IET step and to study the dependence of the decarboxylation step onto the structure of the starting substrate. We adopted a DFT-based method, by employing the ωB97xD functional and the def2TZV basis set, as implemented in the G16 software.[21] Solvent effects were included with an implicit model (methanol bulk) via single point calculations, as detailed in the Supporting Information. Notably, given the open-shell nature of several of the key

---

Table 2. Photochemistry of 3-(4-chlorophenyl)-2,2-dimethylpropionic acid **1b** in polar media.[a]
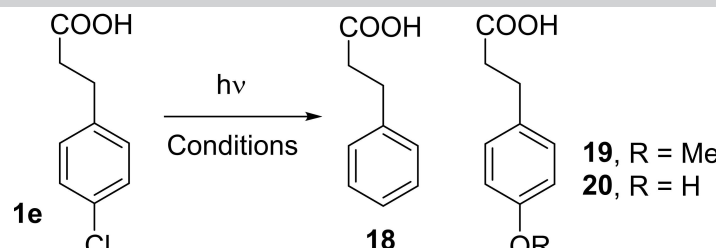

Entry	Conditions [Φ_{-1}][b]	Time [min]	**1b** Consumption [%]	Products, yield [%][c]
1	MeOH (0.02)	120	63	**10**, 75; **11**, 16
2	MeOH + Cs_2CO_3 (1 equiv.) (0.03)	120	65	**10**, 51; **11**, 12; **13**, 11; **14**, 5; **15**, traces[d]
3	PBS[e] (0.12)	120	100	**10**, 68; **12**, 31; **15**, traces[d]

[a] Irradiations were performed at 254 nm (8×15 W low pressure Hg vapor lamps) on a nitrogen-saturated 0.01 M solution of **1b** in the examined solvent. [b] Determined at λ = 254 nm. [c] Yields based on consumed **1b**. [d] Compound **15** detected by GC/MS analysis. [e] Phosphate buffer solution (PBS) 0.05 M, pH = 7.3.

Chemistry–A European Journal

Research Article
doi.org/10.1002/chem.202200313

Chemistry Europe
European Chemical
Societies Publishing

Table 3. Photochemistry of 3-(4-chlorophenyl)-2-methylpropionicc acid **1 c** and 3-(2-chlorophenyl)-2-methylpropionic acid **1 d** in polar media.[a]

1c, 4-Cl
1d, 2-Cl

$h\nu$ / Conditions → **16** **17**

Entry	Compound	Conditions $[\Phi_{-1}]$[b]	Time [min]	1 c/1 d Consumption [%]	Products, yield [%][c]
1	**1 c**	MeOH (0.02)	120	73	**16**, 82
2	**1 c**	MeOH + Cs$_2$CO$_3$ (1 equiv.) (0.03)	120	80	**16**, 98
3	**1 d**	MeOH (0.07)	60	100	**16**, 85
4	**1 d**	MeOH + Cs$_2$CO$_3$ (1 equiv.) (0.07)	60	100	**16**, 57
5	**1 d**[d]	PBS[e] + 5 % MeCN (0.04)	120	80	**16**, 56; **17**, 26

[a] Irradiations were performed at 254 nm (8×15 W low pressure Hg vapor lamps) on a nitrogen-saturated 0.01 M solution of **1 c** or **1 d** in the examined solvent. [b] Determined at $\lambda = 254$ nm. [c] Yields based on consumed **1 c** or **1 d**. [d] 5×10^{-3} M **1 d**. [e] Phosphate buffer solution (PBS) 0.05 M, pH = 7.3.

Table 4. Photochemistry of 3-(4-chlorophenyl)propionic acid **1 e** in polar media.[a]

1e

$h\nu$ / Conditions → **18**

19, R = Me
20, R = H
OR

Entry	Conditions $[\Phi_{-1}]$[b]	Time [min]	1 e Consumption [%]	Products, yield [%][c]
1	MeOH (0.04)	120	75	**18**, 29; **19**, 8
2	MeOH + Cs$_2$CO$_3$ (1 equiv.) (0.05)	120	65	**18**, 77; **19**, 23
3	PBS [d] + 5 % MeCN (0.07)	120	80	**18**, 24; **20**, 41

[a] Irradiations were performed at 254 nm (8×15 W low pressure Hg vapor lamps) on a nitrogen-saturated 0.01 M solution of **1 e** in the examined solvent. [b] Determined at $\lambda = 254$ nm. [c] Yields based on consumed **1 e**. [d] Phosphate buffer solution (PBS) 0.05 M, pH = 7.3.

intermediates, the stability of the obtained wavefunction has always been carefully checked and a re-optimization was performed if an instability was detected (see Supporting Information for full details).

At the beginning of our study, we investigated the detachment of the chlorine atom from the ground state (S_0) and the lowest lying triplet excited state (T_1) in carboxylic acids **1 a**, **1 e** (taken as examples) and the complete set of carboxylate anions **1′a–e**. Very similar results have been obtained for the different structures investigated, as showcased in Figure 2, where the data for **1 a** (part a) and **1 e** (part b) and the corresponding carboxylate anions **1′a** (part c) and **1′e** (part d) have been reported. Thus, Ar–Cl bond cleavage in the S_0 state requires a huge amount of energy (>40 kcal mol^{-1} to elongate the Ar–Cl bond of 0.7 Å), as demonstrated by the steep profile of the corresponding potential energy surfaces (PESs; blue line with square symbols in Figures 2a–d). On the other hand, the typical out-of-plane arrangement of the Cl atom in the optimized triplet state geometries was observed (see the top structures reported in Figures 2a–d), with chlorine detachment easily occurring (see the flat profile of T_1 PESs, red line with circle

symbols): in this case the elongation of the Ar–Cl bond up to ca. 3.0 Å is accompanied by a modest energy increase, ranging from 3.5 to 11.7 for **1′a** and **1 e**, respectively. Furthermore, it can be observed that the Ar–Cl cleavage in all the investigated T_1 states occurs through a heterolytic pathway to afford a triplet aryl cation and the chloride anion ($^3Ar^+ + Cl^-$), since a marked negative charge localization is apparent upon C–Cl bond elongation (e.g., in the case of **1 a**, the chlorine atom at the equilibrium geometry of the T_1 state shares a negative charge equal to -0.24, that shifts to -0.69 upon elongation of the C–Cl bond to ca. 3.0 Å; see Figure 2a). Indeed, the negative charge localization in the case of **1 a** is larger than for **1 e**, in accordance with the different electronic character of the two aromatic derivatives (the former is expected to be more electron-rich than the latter). In addition, when moving from the carboxylic acids **1 a/1 e** to the corresponding carboxylate anions **1′a/1′e**, an increase in the localization of the negative charge on the chlorine atom of the respective triplet states is consistently observed. The data related to **1′b–d** reveal essentially the same behavior (see Figure S2 in the Supporting Information). Overall, this is a clear indication that the formation
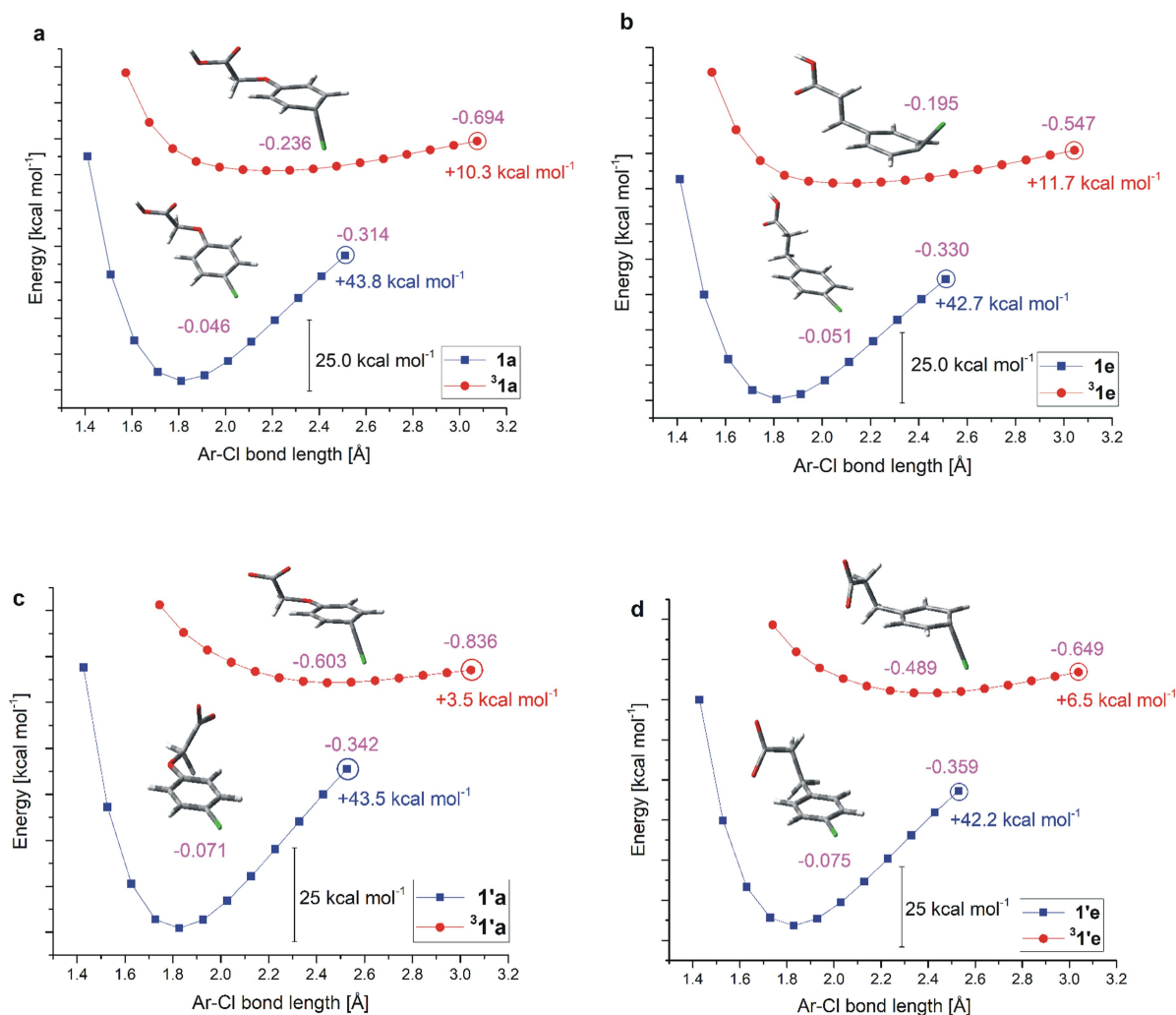
Chemistry–A European Journal

Research Article
doi.org/10.1002/chem.202200313

Chemistry Europe
European Chemical
Societies Publishing

Figure 2. Potential energy surfaces (PESs) of the S_0 (blue line with square symbols) and T_1 (red line with circle symbols) states for: **1a** (part a), **1e** (part b), **1'a** (part c), **1'e** (part d) at the ωB97xD/def2TZV level of theory in bulk methanol. The reported structures are the optimized geometries for the S_0 (lower part) and T_1 (upper part) states. The values reported in magenta do refer to the charge localized at the chlorine atom (green) at the equilibrium geometry and upon elongation of the C—Cl bond (evaluated on the last point of each curve). The values reported in blue (for S_0 states) and red (for T_1 states) refer to the energy change associated with the last point with respect to the minimum for each curve.

of a triplet phenyl cation is feasible in all cases and does not depend on the protonation state of the substrate.

Next, we shifted our attention on the feasibility of the claimed IET step. To do so, we adopted a previously reported theoretical method to calculate the redox potentials of organic derivatives.[22,23] Our aim was to predict the oxidation capability of triplet phenyl cations deriving from substrates **1'a** and **1'e**, taken as reference compounds. Accordingly, we estimated the redox potential of the $^3Ar^+/Ar^•$ redox couple. We postulated that such redox potential is essentially dictated by the substituents attached to the aromatic nucleus, so we adopted the triplet *p*-methoxyphenyl cation/*p*-methoxyphenyl radical and the triplet *p*-ethylphenyl cation/*p*-ethylphenyl radical, respectively, as convenient surrogates for determining the desired parameters in **1'a** and **1'e**. Table 5 gathers the obtained data, showcasing that the alkyl-substituted phenyl cation is ca. 600 mV more oxidizing than the methoxy-substituted derivative

(entries 1, 2), as expected based on the electronic effect imparted by such substituents on the aromatic nucleus.

We also reasoned that triplet phenyl cations share a peculiar electronic structure, with the two unpaired electrons located in non-interacting orbitals, respectively, in a sp^2-hybridized orbital at the dicoordinated carbon (aryl radical character) and delocalized over the entire π system (aromatic radical cation character).[24] Accordingly, the calculated redox potentials for **1'a** and **1'e** should parallel the oxidation potential of the parent compounds (anisole and ethylbenzene) to afford the corresponding radical cations. Our hypothesis was fully confirmed, as apparent by comparing the data in entries 3 and 4 with those in entries 1 and 2, respectively. The validity of the implemented theoretical approach is corroborated by the close similarity of the simulated data with the experimental ones available in the literature (Table 5).

Chemistry–A European Journal

Research Article
doi.org/10.1002/chem.202200313

Chemistry Europe
European Chemical
Societies Publishing

Table 5. Calculated/experimental potentials of redox couples relevant to the rationalization of the proposed IET step.

Entry	Redox couple	Calculated redox potentials in MeCN [V vs. SCE][a]	Experimental redox potentials in MeCN [V vs. SCE]
1	3 OMe ⟍ OMe	+1.68	–
2	3 Et ⟍ Et	+2.27	–
3	OMe ⟍ OMe	+1.76	+1.81[25]
4	Et ⟍ Et	+2.33	+2.14[26]

[a] The reported values have been calculated at the M06-2X/6-31+G(d,p) level of theory in MeCN bulk, as reported in Ref. [22].

Figure 3. Spin density plots for intermediates ³21⁺ arising from 1a (part a) and 1e (part b), and intermediates ³22 arising from 1′a (part c) and 1′e (part d), as determined from ωB97xD/def2TZV calculations in bulk methanol.

Turning to the key IET step relevant to this work, the calculated redox potentials of triplet phenyl cations have to be compared with those of typical carboxylate anions. In particular, there is a little dependence on the actual structure of the group attached to the carboxylate group, with redox potentials in the +1.26 V (pivalate anion) to +1.47 V (acetate anion) vs. SCE range, as previously reported.[22] As apparent from these data, in any case, the predicted IET may occur through an overall exergonic step since the oxidation potentials of the phenyl cations formed in this work are always > ca. +1.7 V vs. SCE.

We next investigated the geometries and electronic structures of the triplet phenyl cations ³21⁺a–e and triplet diradicals ³22a–e (see selected examples in Figure 3) arising via chloride anion detachment from 1a–e and 1′a–e, respectively. We found that the latter parameter dramatically depends on the protonation state of the carboxylic acid group, as shown in Figure 3, wherein the spin density plots of the intermediates resulting from 1a/1e (upper part) and 1′a/1′e (lower part) are reported. Thus, it is apparent that the free acids feature the typical electronic structure of a triplet phenyl cation, in accordance with the radical/radical cationic description reported above. On the other hand, in the latter case a diradical structure is easily detected, with the two unpaired electrons located, respectively, at the dicoordinated carbon and at the carboxyl group, consistent with the occurrence of the claimed IET step. A rather
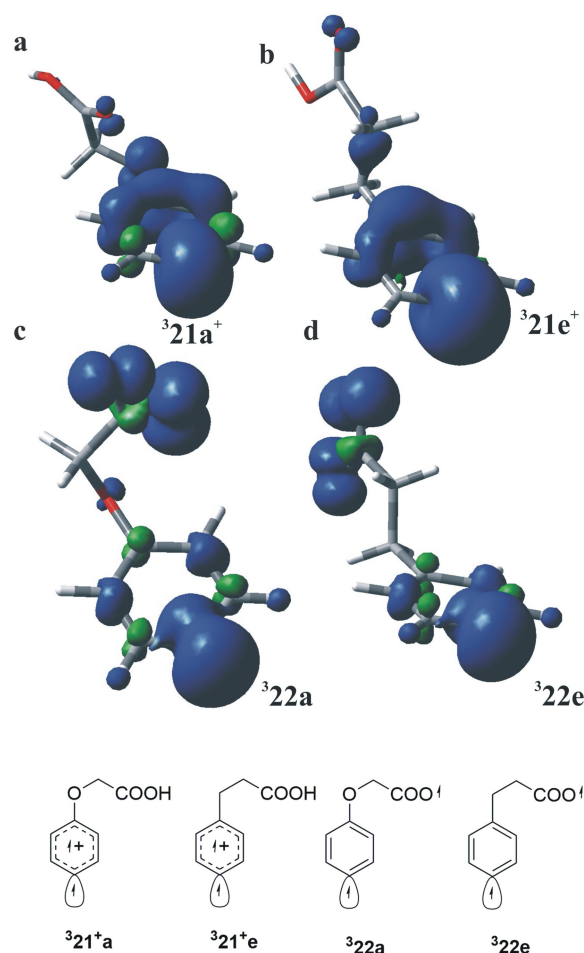
similar situation has been observed for all the remaining substrates tested (see Figure S3).

To have more information on the reactivity pattern offered by such intermediates, we optimized the geometries of all the phenyl cations and diradicals arising from 1a–e and 1′a–e, respectively, in the corresponding singlet spin manifold and calculated the singlet-triplet (S–T) gap. The results are shown in Figure 4, where a positive bar indicates that the singlet state is more stable than the triplet and vice versa. In all cases, the singlet phenyl cations (¹21⁺, Scheme 3) arising from 1a–e are more stable than the corresponding triplet congeners (³21⁺) by ca. 10–15 kcal mol⁻¹, with the only exception of the 4-methoxyphenyl cation, where the two spin states are almost isoenergetic (the S–T gap is very small, with the triplet more stable than the singlet by a mere 0.5 kcal mol⁻¹). On the other hand, all the diradical species 22 arising from 1′a–e show a similar behavior with all the triplets slightly more stable (ca. 1.0 kcal mol⁻¹) than the corresponding singlets.

The possibility to observe a decarboxylation step from either the singlet or triplet diradical species 22 (arising from 1′a–e) has been modeled next. To this end, we located the

Chemistry–A European Journal

Research Article
doi.org/10.1002/chem.202200313

Chemistry Europe
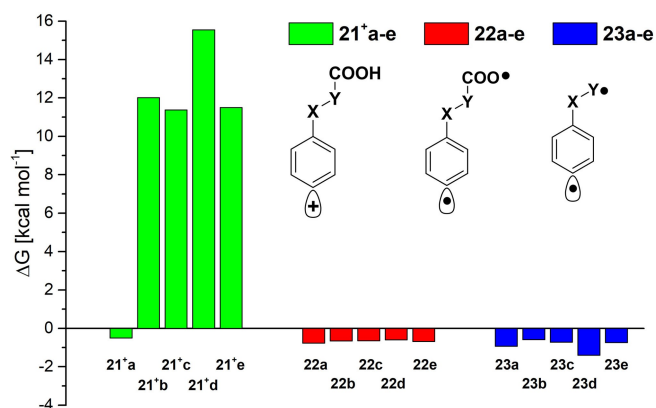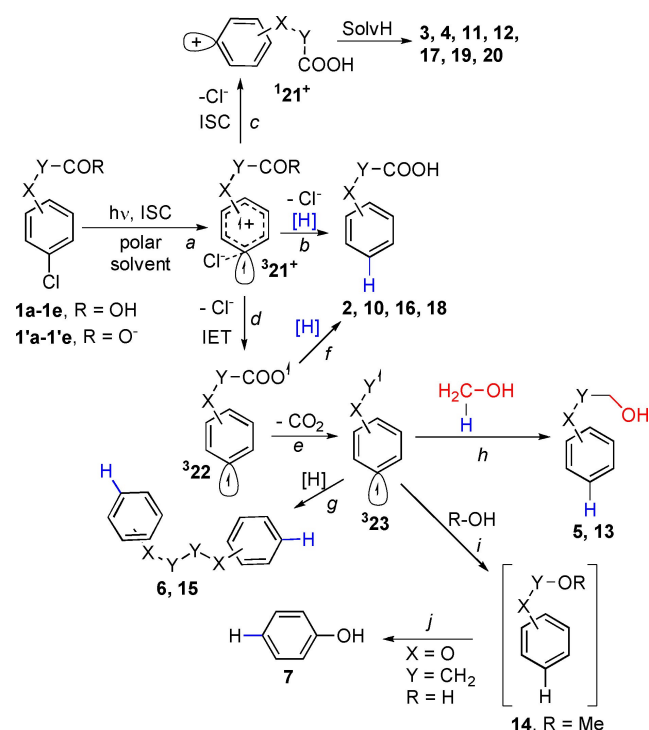European Chemical
Societies Publishing

Figure 4. Singlet-triplet (S–T) gaps for intermediates **21$^+$** (green bars), **22** (red bars) and **23** (blue bars) as determined from ωB97xD/def2TZV calculations in bulk methanol. A positive bar indicates a singlet ground-state intermediate.

Table 6. Ease of CO_2 detachment from intermediates **22** expressed as Gibbs free energy change ($\Delta G^{\ddagger}$) calculated at the ωB97xD/def2TZV level of theory in methanol bulk.[a]

Transition state	Singlet spin manifold, $\Delta G^{\ddagger}$ [kcal mol^{-1}]	Triplet spin manifold, $\Delta G^{\ddagger}$ [kcal mol^{-1}]
22-TSa	0.65	0.94
22-TSb	1.94	1.85
22-TSc	1.12	1.00
22-TSd	1.57	1.45
22-TSe	5.67	5.56

[a] The values reported have been determined by taking the appropriate energy difference between the energy of the TS (**22-TS**) and that of the corresponding parent intermediate **22**.

Scheme 3. Proposed mechanistic scenario for the photoreactivity of compounds **1 a–e**.

relevant transition states (tagged as **22-TS**), describing the C–COO$^{\bullet}$ bond cleavage and the corresponding $\Delta G^{\ddagger}$ are reported in Table 6. The nature of the TSs has been fully characterized through vibrational analysis and the corresponding IRC plots (15 points in both forward/reverse directions) are reported in the Supporting Information (see Figure S4), fully confirming that the located TSs describe the desired C–C cleavage. As for the observed energy changes with respect to the parent diradical species **22**, the trend clearly reflects the stability of the diradicals accessible upon CO_2 loss. Accordingly,

the ease of decarboxylation follows the order **22 a** > **22 b** ~ **22 c** ~ **22 d** ≫ **22 e**, independently from the considered spin manifold.

As a final consideration, we wanted to have insight into the hypothetical diradical species arising from the decarboxylation step (intermediates **23** from **1′ a–e**). Accordingly, we optimized such species both in the singlet and the triplet states, thereby calculating the S–T gap. The results of such simulations are reported in Figure 4. As a matter of fact, also in this case, all the diradical species share a very small S–T gap (up to ca. 1.4 kcal mol^{-1}), with the triplets consistently more stable than the corresponding singlets.

Discussion

The experimental and computational evidences point to the mechanistic scenario described in Scheme 3. Each of the chloroaryl-substituted carboxylic acids **1 a–e** tested belongs to the class of (slightly) electron-rich chlorobenzenes (the σ_p^+ values of the OMe and the CH_2CH_2COOH groups, taken as the reference, are −0.78 and −0.07, respectively).[27] These compounds, upon excitation in polar solvents, are known to lose the chloride anion from the excited triplet state[28] to form the intimate ion pair triplet phenyl cation (^{3}**21$^+$**/chloride anion, path a).[8d] The efficiency of the photoreaction is modest, since Φ_{-1} did not exceed 0.1 in most cases. The occurrence of the reaction from the triplet state is confirmed by acetone-sensitized experiments that gave roughly the same product distribution observed under non-sensitized conditions (see Table 1, compare entries 3 and 4). At this stage, a different chemistry from the carboxylic acids and the corresponding carboxylate anions takes place. In the former case, the typical reactivity of a triplet phenyl cation was observed, mainly leading to dechlorinated derivatives via hydrogen atom abstraction from the solvent (path b).[17] This is apparent when the reaction is carried out in an excellent hydrogen-donating solvent, such as iPrOH (Table 1).[29] Since phenyl cations may exist both in the singlet and in the triplet state, an intersystem crossing may take place between the two forms depending on their relative energies. As shown in Figure 4, the singlet cations are consistently more stable than the triplets (except for **21 a$^+$**) allowing the formation of ^{1}**21$^+$** (path c). In nucleophilic solvents,

Chem. Eur. J. **2022**, 28, e202200313 (8 of 11)

© 2022 The Authors. Chemistry - A European Journal published by Wiley-VCH GmbH

Chemistry–A European Journal

Research Article
doi.org/10.1002/chem.202200313

**Chemistry
Europe**

European Chemical
Societies Publishing

such as MeOH and water, solvent addition occurred to form the corresponding phenols or anisoles, accordingly. The amount of solvolysis products increased when the reaction was carried out in a highly polar solvent (such as aqueous PBS) due to the high stability imparted by the medium to the photogenerated cation.[30]

This work again confirms that triplet phenyl cations $^3\mathbf{21}^+$ have a radical cationic nature and we demonstrate a noteworthy similarity with the radical cations obtained via monoelectronic oxidation of the corresponding arenes. Nonetheless, the typical benzylic deprotonation of such intermediates was not observed here, as previously reported in the case of radical cations of alkyl benzenes[31] and 4-phenylbutanoic acids.[32]

The feasibility of an IET step between the radical cationic site of the triplet phenyl cations and the COO^- group was estimated by calculating the oxidation capability of the aromatic nucleus (Table 5). Thus, it was demonstrated for the first time that the triplet p-methoxyphenyl cation and the anisole radical cation share a similar redox potential (Table 5), confirming again that the two radical sites in $^3\mathbf{21}^+$ are independent from each other. With this important notion in our hand, we could rule out an IET from the intermediates $^3\mathbf{21}^+$ having a protonated COOH group, since this moiety is difficult to oxidize (the $E_{1/2}^{OX}$ of phenylacetic acid is $+2.51$ V vs. SCE).[33]

The situation dramatically changes, however, in the case of carboxylates $\mathbf{1'a}$–$\mathbf{e}$. Irradiation of $\mathbf{1'a}$ in basic MeOH led exclusively to products lacking the carboxylic group, pointing to an IET followed by decarboxylation (Scheme 3, paths d, e) to give diradical $^3\mathbf{23a}$. The exergonicity of the IET step is corroborated by the smooth oxidizability of the carboxylate group ($< +1.5$ V vs. SCE) compared to its protonated form. Moreover, the ΔG^+ of the decarboxylation step in $^3\mathbf{22a}$ is very low (less than 1 kcal mol^{-1}) independently of the multiplicity of the diradical (Table 6). In aqueous PBS the decarboxylation is not complete, however, since dechlorinated $\mathbf{2}$ and the water-incorporating product $\mathbf{3}$ were likewise formed. In the latter medium, IET seems to have a less important role compared to basic MeOH allowing some phenyl cation chemistry. This contrasts with the exergonicity of the IET that should funnel the reactivity exclusively into path d to give $^3\mathbf{22a}$. A possible explanation is that cation $^3\mathbf{21a}^+$ is not "bare", but rather exists as an intimate ion pair with the leaving group (the chloride anion). Such interaction hampers the IET step and, accordingly, prevents decarboxylation.[8d] Moreover, the stability of phenyl cations strongly increased when enhancing the proticity of the medium.[30] The presence of a modest amount of glucose (0.05 M, a good hydrogen donor) slightly increased the amount of photodechlorinated $\mathbf{2}$, but did not affect carbon dioxide loss (Table 1), as previously demonstrated in related cases.[9]

The next crucial point is the reactivity of diradical $^3\mathbf{23a}$. Such diradical has not been formed previously, even under thermal conditions, so its behavior is unprecedented. The radical nature of this intermediate was however confirmed by both deuteration experiments and the $t$butyl acrylate-trapping experiment to give adducts $\mathbf{8}$ and $\mathbf{9}$ in a low yield. Albeit the formation of dimers (such as $\mathbf{6}$, path g) is reasonable, these diradicals, similarly to α,n-DHTs, are surprisingly able to incorporate a

molecule of the reaction medium (whether MeOH or water). These new species show again a diradical and a polar dichotomy, in analogy with α,n-DHTs.[8b] In the former case (path h), compound $\mathbf{5}$ was obtained via C–C bond formation. In the latter case (path i) a C–O bond was formed and the addition of water onto the diradical gave a hemiacetal (see compound $\mathbf{14}$) that readily hydrolyzed to phenol $\mathbf{7}$ (path j). Notably, a double hydrogen abstraction by $^3\mathbf{23a}$ has not been observed, thus pointing out the great difference in stability between the aryl and the α-oxy radical sites in this intermediate. Shifting to compound $\mathbf{1b}$, the decarboxylation extent was rather limited, despite the strong basic conditions (Table 2). This fact clearly points out that the stability of the diradical $^3\mathbf{23b}$ is the driving force for CO_2 detachment from $^3\mathbf{22b}$. Indeed, the 1-phenoxymethyl-like radical formed from $\mathbf{1a}$ is probably more stable than the tertiary radical formed from $\mathbf{1b}$. In the case of compounds $\mathbf{1c}$–$\mathbf{e}$, the decarboxylation of the generated diradicals $^3\mathbf{22c}$–$\mathbf{e}$ is completely prevented due to the high value of the ΔG^+ of decarboxylation (Table 6), pointing to the poor stability of the resulting $^3\mathbf{23c}$–$\mathbf{e}$.

An intriguing question raises on the actual involvement of diradicals $^3\mathbf{22}$ in the photochemistry of $\mathbf{1a}$–$\mathbf{e}$. Specifically, a double hydrogen abstraction from such species via path f is an alternative route to the formation of photodechlorinated derivatives via path b (Scheme 3). The hydrogen abstraction in path f is largely favored by the strength of the C–H/O–H bonds formed (the strength of the Ar–H bond in benzene is ca. 113 kcal mol^{-1} and that of CH$_3$CH$_2$COO–H bond is 106.4 kcal mol^{-1}).[34] The intermediacy of $^3\mathbf{22}$ (and, accordingly, the occurrence of IET at the $^3\mathbf{21}^+$ level) is confirmed in the photoreaction of $\mathbf{1a}$, wherein the chemistry of $^3\mathbf{23}$ via paths d and e has been observed (at least in basic MeOH). The IET pathway should in principle operates with the same efficiency also in the photoreactions of $\mathbf{1b}$–$\mathbf{e}$ (see also Table 5) and an exclusive chemistry from $^3\mathbf{22}$ or $^3\mathbf{23}$ should result. However, this seems in contrast with the consistent presence of photo-substitution products (diagnostic of the reactivity of $^1\mathbf{21}^+$) in those cases. We thus suggest that, since phenyl cations $^3\mathbf{21}^+\mathbf{b}$–$\mathbf{e}$ obtained from $\mathbf{1b}$–$\mathbf{e}$ are less stable than that formed from $\mathbf{1a}$ (due to the lack of a stabilizing OR group; compare the energy changes for chlorine detachment in the triplet states from $\mathbf{1a}$ and $\mathbf{1e}$; Figure 2), the ion couples $^3\mathbf{21}^+\mathbf{b}$–$\mathbf{e}$/Cl$^-$ have a role, therefore driving the reactivity to paths b, c at the expenses of IET. The stabilizing effect of water seems likewise to favor a phenyl cation chemistry.

Conclusions

This work demonstrates that new classes of diradicals may be formed in a very mild way by having recourse to an IET occurring in photogenerated triplet phenyl cations having oxidizable moieties tethered to the aromatic nucleus by a suitable spacer. The feasibility of the IET may be predicted by calculations and tuned at will by choosing the substituents of the aromatic nucleus (electron-donating groups can lower the oxidation capability) and the redox potential of the oxidizable

Chemistry–A European Journal

Research Article
doi.org/10.1002/chem.202200313

Chemistry Europe
European Chemical
Societies Publishing

moiety. In addition, the latter group may induce a diradical cascade, if lost as a stable molecule after the IET. In the present work, the lack of the elimination of the electrofugal group may generate in the same substrate two aggressive radical sites (an aryl radical and a carbonyloxy radical), capable to abstract hydrogen atoms from the medium.

More investigations are, however, needed to prove if these diradicals may have a role as antitumoral species by abstracting hydrogen atoms from DNA in analogy with the mechanism of action of enediyne antitumor antibiotics.

Experimental Section

Irradiations were performed by using nitrogen-purged solutions in quartz tubes in a multi-lamp reactor fitted with 10×15 W phosphor-coated Hg lamps (maximum of emission at 310 nm) or with 10×15 W low-pressure Hg lamps (maximum of emission at 254 nm). Quantum yields were measured at 254 nm (1 Hg lamp, 15 W). The reaction course was followed by both GC and HPLC analyses.

Conflict of Interest

The authors declare no conflict of interest.

Data Availability Statement

The data that support the findings of this study are available in the supplementary material of this article.

[1] a) M. Abe, *Chem. Rev.* **2013**, *113*, 7011–7088; b) T. Stuyver, B. Chen, T. Zeng, P. Geerlings, F. De Proft, R. Hoffmann, *Chem. Rev.* **2019**, *119*, 11291–11351.

[2] a) C. Raviola, S. Protti, D. Ravelli, M. Fagnoni, *Chem. Soc. Rev.* **2016**, *45*, 4364–4390; b) I. V. Alabugin, W.-Y. Yang, R. Pal, in *CRC Handbook of Organic Photochemistry and Photobiology, 3rd Edition* (Eds: A. Griesbeck, M. Oelgemoeller, F. Ghetti), CRC press, Boca Raton, **2012**, pp. 549–592.

[3] a) U. Galm, M. H. Hager, S. G. Van Lanen, J. Ju, J. S. Thorson, B. Shen, *Chem. Rev.* **2005**, *105*, 739–758; b) A. L. Smith, K. C. Nicolaou, *J. Med. Chem.* **1996**, *39*, 2103–2117; c) K. C. Nicolau, A. L. Smith, *Acc. Chem. Res.* **1992**, *25*, 497–503.

[4] a) A. Albini, M. Fagnoni in *Photochemically-generated intermediates in synthesis.* John Wiley & Sons, Hoboken, **2013**, pp 131–167; b) D. Ravelli, S. Protti, M. Fagnoni, *Chem. Rev.* **2016**, *116*, 9850–9913.

[5] a) P. Wessig in *CRC Handbook of Organic Photochemistry and Photobiology, 2nd edition* (Eds: F. Lenci, W. Horspool) CRC Press, Boca Raton, **2004**, pp. 57–1-57–20; b) P. J. Wagner in *CRC Handbook of Organic Photochemistry and Photobiology, 2nd edition* (Eds: F. Lenci, W. Horspool) CRC Press, Boca Raton, **2004**, pp. 58–1-58–70; c) P. J. Wagner in *Molecular and Supramolecular Photochemistry. Synthetic Organic Photochemistry* (Eds: A. G. Griesbeck, J. Mattay), Vol. 12, Marcel Dekker, New York, **2005**, pp. 11–40; d) P. Wessig, O. Mühling in *Molecular and Supramolecular Photochemistry. Synthetic Organic Photochemistry* (Eds: A. G. Griesbeck, J. Mattay) Vol. 12, Marcel Dekker, New York, **2005**, pp. 41–88; e) M. A. Garcia-Garibay, L. M. Campos in *CRC Handbook of Organic Photochemistry and Photobiology, 2nd edition* (Eds: F. Lenci, W. Horspool) CRC Press, Boca Raton, **2004**, pp. 48–1-48–41; f) S. Majhi *Photochem. Photobiol. Sci.* **2021**, *20*, 1357–1378.

[6] T. Kusakabe, M. Uesugi, Y. Sugiura, *Biochemistry* **1995**, *34*, 9944–9950.

[7] a) A. G. Myers, M. E. Kort, M. J. Hammond, *J. Am. Chem. Soc.* **1997**, *119*, 2965–2972; b) A. G. Myers, C. A. Parrish, *Bioconjugate Chem.* **1996**, *7*, 322–331.

[8] a) S. Protti, D. Ravelli, B. Mannucci, A. Albini, M. Fagnoni, *Angew. Chem. Int. Ed.* **2012**, *51*, 8577–8580; *Angew. Chem.* **2012**, *124*, 8705–8708; b) C. Pedroli, D. Ravelli, S. Protti, A. Albini, M. Fagnoni, *J. Org. Chem.* **2017**, *82*, 6592–6603; c) C. Raviola, D. Ravelli, S. Protti, M. Fagnoni, *J. Am. Chem. Soc.* **2014**, *136*, 13874–13881; d) D. Ravelli, S. Protti, M. Fagnoni, *J. Org. Chem.* **2015**, *80*, 852–858.

[9] S. Crespi, S. Protti, D. Ravelli, D. Merli, M. Fagnoni, *J. Org. Chem.* **2017**, *82*, 12162–12172.

[10] S. Montanaro, D. Ravelli, D. Merli, D. Fagnoni, A. Albini, *Org. Lett.* **2012**, *14*, 4218–4221.

[11] L. Di Terlizzi, F. Roncari, S. Crespi, S. Protti, M. Fagnoni, *Photochem. Photobiol. Sci.* **2022**, *21*, https://doi.org/10.1007/s43630-021-00119-6.

[12] a) J. Blumberger, *Chem. Rev.* **2015**, *115*, 11191–11238; b) H. R. Williamson, B. A. Dow, V. L. Davidson, *Bioorg. Chem.* **2014**, *57*, 213–221.

[13] See for example: a) E. Fasani, M. Fagnoni, D. Dondi, A. Albini, *J. Org. Chem.* **2006**, *71*, 2037–2045; b) J. J. Murphy, D. Bastida, S. Paria, M. Fagnoni, P. Melchiorre, *Nature* **2016**, *532*, 218–222.

[14] a) G. L. Closs, J. R. Miller, *Science* **1988**, *240*, 440–447; b) J. W. Verhoeven, *Advances in Chemical Physics, Volume 106, Election Transfer-From Isolated Molecules to Biomolecules, Part One* (Eds: J. Jortner, M. Bixon) Series Editors I. Prigogine, S. A. Rice. John Wiley & Sons, Inc, **1999**; c) S. Antonello, F. Maran, *Chem. Soc. Rev.* **2005**, *34*, 418–428.

[15] Y. Okada, K. Chiba, *Chem. Rev.* **2018**, *118*, 4592–4630.

[16] M. Oelgemöller, A. G. Griesbeck, *J. Photochem. Photobiol. C* **2002**, *3*, 109–127.

[17] V. Dichiarante, S. Protti, M. Fagnoni, *J. Photochem. Photobiol. A* **2017**, *339*, 103–113.

[18] a) M. Bietti, M. Salamone, *J. Org. Chem.* **2005**, *70*, 10603–10606; b) C. S. A. Antunes, M. Bietti, G. Ercolani, O. Lanzalunga, M. Salamone, *J. Org. Chem.* **2005**, *70*, 3884–3891; c) M. Bietti, A. Calcagni, D. O. Cicero, R. Martella, M. Salamone, *Tetrahedron Lett.* **2010**, *51*, 4129–4131.

[19] M. Ando, S. Yoshiike, T. Suzuki, T. Ichimura, T. Okutsu, M. Ueda, H. Horiuchi, H. Hiratsuka, A. Kawai, K. Shibuya, *J. Photochem. Photobiol. A* **2005**, *174*, 194–198.

[20] a) R. S. Davidson, K. Harrison, P. R. Steiner, *J. Chem. Soc. C* **1971**, 3480–3482; b) F. Karasu, N. Arsu, S. Jockusch, N. J. Turro, *Macromoecules.* **2009**, *42*, 7318–7323.

[21] Gaussian 16, Revision C.01, M. J. Frisch, G. W. Trucks, H. B. Schlegel, G. E. Scuseria, M. A. Robb, J. R. Cheeseman, G. Scalmani, V. Barone, G. A. Petersson, H. Nakatsuji, X. Li, M. Caricato, A. V. Marenich, J. Bloino, B. G. Janesko, R. Gomperts, B. Mennucci, H. P. Hratchian, J. V. Ortiz, A. F. Izmaylov, J. L. Sonnenberg, D. Williams-Young, F. Ding, F. Lipparini, F. Egidi, J. Goings, B. Peng, A. Petrone, T. Henderson, D. Ranasinghe, V. G. Zakrzewski, J. Gao, N. Rega, G. Zheng, W. Liang, M. Hada, M. Ehara, K. Toyota, R. Fukuda, J. Hasegawa, M. Ishida, T. Nakajima, Y. Honda, O. Kitao, H. Nakai, T. Vreven, K. Throssell, J. A. Montgomery, Jr., J. E. Peralta, F. Ogliaro, M. J. Bearpark, J. J. Heyd, E. N. Brothers, K. N. Kudin, V. N. Staroverov, T. A. Keith, R. Kobayashi, J. Normand, K. Raghavachari, A. P. Rendell, J. C. Burant, S. S. Iyengar, J. Tomasi, M. Cossi, J. M. Millam, M. Klene, C. Adamo, R. Cammi, J. W. Ochterski, R. L. Martin, K. Morokuma, O. Farkas, J. B. Foresman, D. J. Fox, Gaussian, Inc., Wallingford CT, 2016.

[22] H. G. Roth, N. A. Romero, D. A. Nicewicz, *Synlett* **2016**, *27*, 714–723.

[23] For additional details about conversion of computational results in redox potentials, see also: A. A. Isse, A. Gennaro, *J. Phys. Chem. B* **2010**, *114*, 7894–7899.

[24] S. Lazzaroni, D. Dondi, M. Fagnoni, A. Albini, *J. Org. Chem.* **2008**, *73*, 206–211.

[25] T. Tajima, A. Nakajima *J. Am. Chem. Soc.* **2008**, *130*, 10496–10497.

[26] S. Fukuzumi, J. Yuasa, N. Satoh, T. Suenobu, *J. Am. Chem. Soc.* **2004**, *126*, 7585–7594.

[27] C. Hansch, A. Leo, R. W. Taft, *Chem. Rev.* **1991**, *91*, 165–195.

[28] C. Raviola, D. Ravelli, S. Protti, A. Albini, M. Fagnoni, *Synlett* **2015**, *26*, 471–478.

[29] V. Dichiarante, M. Fagnoni, A. Albini, *Green Chem.* **2009**, *11*, 942–945.

[30] a) V. Canevari, M. Fagnoni, P. Bortolus, A. Albini, *ChemSusChem* **2011**, *4*, 98–103; b) I. Manet, S. Monti, G. Grabner, S. Protti, D. Dondi, V. Dichiarante, M. Fagnoni, A. Albini, *Chem. Eur. J.* **2008**, *14*, 1029–1039.

[31] R. Zhou, H. Liu, H. Tao, X. Yu, J. Wu, *Chem. Sci.* **2017**, *8*, 4654–4659 and references therein.

[32] T. Duhamel, K. Muñiz, *Chem. Commun.* **2019**, *55*, 933–936.

[33] L. Capaldo, L. Buzzetti, D. Merli, M. Fagnoni, D. Ravelli, *J. Org. Chem.* **2016**, *81*, 7102–7109.

[34] Y.-R. Luo, *Comprehensive Handbook of Chemical Bond Energies*; CRC Press, Boca Raton, 2007.